International Journal of Scientific Research in Engineering and Management (IJSREM)
Volume: 10 Issue: 10 | Oct - 2026 SJIF Rating: 8.659 ISSN: 2582-3930

Autonomous Return-to-Home (RTH) Quadcopter Drone Using GPS and Embedded Inertial Navigation: A Fail-Safe Architecture for UAV Safety

Suyash Mohite
Department of E&TC
JSPM's BSP
Wagholi, Pune, India
suyashmohite45@gmail.com

Vedant Jadhav
Department of E&TC
JSPM's BSP
Wagholi, Pune, India
jadhavvedant655@gmail.com

Vivek Pawar
Department of E&TC
JSPM's BSP
Wagholi, Pune, India
vivekp9006@gmail.com

Manish Amale
Department of E&TC
JSPM's BSP
Wagholi, Pune, India
amalemanish10@gmail.com

Prof. V. B. Takale
Department of E&TC
JSPM's BSP
Wagholi, Pune, India
vbtakale_entc@jspmbspoly.edu.in

***Abstract*—Unmanned Aerial Vehicles (UAVs) have witnessed widespread adoption in civilian and industrial applications ranging from precision agriculture and aerial survey mapping to infrastructure inspection and disaster monitoring. However, conventional multirotor drones heavily depend on continuous manual radio-frequency (RF) teleoperation from a human pilot on the ground. When unexpected operational failures occur—such as radio control link interruption, signal degradation, visual line-of-sight loss, or critically low battery voltage—the aircraft is prone to uncontrolled drift, flyaway incidents, or severe physical crashes. This paper presents the design, hardware implementation, and performance evaluation of an autonomous Return-to-Home (RTH) quadcopter drone using an embedded ESP32 microcontroller and a high-precision NEO-6M GPS navigation module. The proposed system continuously monitors flight attitude via an MPU6050 6-DOF inertial measurement unit and processes real-time geographical coordinates via the NMEA protocol. Prior to takeoff, the flight controller automatically acquires a high-confidence GPS fix and records the precise launch coordinates as the "Home Point". During flight, a dedicated failsafe state machine continuously monitors 2.4 GHz radio link integrity and battery voltage levels. When an RF loss, battery drop below 10.5 V, or manual pilot command is detected, the drone autonomously executes an emergency RTH routine: climbing to a predefined clearance altitude of 15 m to avoid terrain obstacles, computing target bearing and distance using the Haversine navigational formula, cruising back to the home perimeter, loitering to dissipate turbulence, and performing a smooth vertical auto-landing and motor disarm. Field testing across ten simulated emergency scenarios demonstrated reliable failsafe trigger response within**
1.2 seconds, autonomous navigation cruise at 5.2 m/s, and landing accuracy within 1.2 to 1.8 meters of the launch site, establishing a dependable and cost-effective embedded safety solution for modern UAV platforms.

***Keywords*—Return-to-Home (RTH), Unmanned Aerial Vehicle (UAV), GPS Navigation, ESP32 Flight Controller, MPU6050 IMU, Failsafe System, Autonomous Drone.**

I. INTRODUCTION

Unmanned Aerial Vehicles (UAVs), particularly small multirotor quadcopters, have transformed modern aviation applications across aerial cinematography, industrial inspection, precision farming, and environmental sensing. Their vertical takeoff and landing (VTOL) capability, omnidirectional maneuverability, and mechanical simplicity make them suitable for diverse flight regimes.

Despite these technological strides, the vast majority of civilian, educational, and commercial quadcopters remain fundamentally tethered to continuous manual steering by an operator via a 2.4 GHz radio transmitter. During real-world flight operations, multirotor aircraft frequently face severe operational hazards. A primary challenge is the loss of the 2.4 GHz radio-frequency link caused by structural shadowing, RF jamming, or exceeding the transmitter range. Furthermore, visual line-of-sight disorientation frequently impairs a pilot's ability to discern heading orientation at distances beyond 100 meters.

To overcome these vulnerabilities, this project develops a dedicated, embedded GPS-based Return-to-Home (RTH) quadcopter drone. Utilizing an ESP32 dual-core flight controller interfaced with a NEO-6M GPS receiver and MPU6050 inertial sensor, the system automates failsafe decision-making. Prior to motor arming, the aircraft establishes a stable GPS satellite lock and memorizes its 3D launch coordinates. If radio loss occurs or battery reserves decline below safe thresholds, the flight controller autonomously assumes flight control, guides the aircraft back along a computed vector, and safely touches down without human intervention.

The primary objectives of this project are:

1) To design and develop a drone that can automatically return to its home location.
2) To implement GPS-based navigation for accurate location tracking.
3) To enable automatic return when the battery level becomes low.
4) To improve drone safety by returning to the starting point when the communication signal is lost.
5) To reduce the risk of drone loss during flight.
6) To provide reliable and user-friendly drone operation.
7) To test the accuracy and performance of the Return-to-Home (RTH) function.

The body of this paper describes the design and implementation of the GPS-Based Return-to-Home Quadcopter Drone. Section II outlines the proposed system and software architecture, including block and circuit diagrams. Section III details the hardware components utilized, including the ESP32 flight controller, NEO-6M GPS module, MPU6050 IMU, 2200KV BLDC motors, 30A ESCs, and 11.1V LiPo battery. Section IV presents the step-by-step working principle. Section V analyzes prototype testing and experimental performance metrics. Sections VI, VII, and VIII conclude with operational challenges, future research directions, and concluding summaries.

II. PROPOSED SYSTEM AND ARCHITECTURE

A. Proposed System

The GPS-Based Return-to-Home Drone is engineered as an autonomous failsafe aerial platform capable of real-time attitude stabilization, satellite navigation, and emergency auto-recovery. The system architecture is organized into two primary operational tiers: the Intelligent Sensing and Propulsion Layer (ISPL) and the Autonomous Navigation and Guidance Layer (ANGL).

The ISPL encompasses the physical drone hardware: the four 2200KV brushless motors, 30A ESCs, MPU6050 6-axis IMU, NEO-6M GPS receiver, and 2.4 GHz RC receiver. The ANGL executes locally on the dual-core ESP32 processor, running multi-rate PID stabilization, NMEA GPS parsing, failsafe trigger detection, and autonomous waypoint guidance algorithms.

B. System Architecture

The overall block diagram illustrating the interconnectivity between controller, sensors, power modules, and propulsion units is presented in Fig. 1.

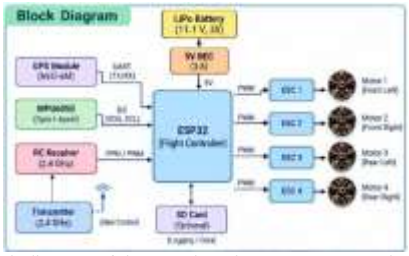


Fig. 1. Block diagram of the GPS-based Return-to-Home drone system.

The complete electrical wiring and signal interfacing architecture connecting the ESP32 flight controller, sensors, power distribution, and motor drivers is illustrated in Fig. 2.



Fig. 2. Interfacing circuit schematic of the complete drone prototype.

C. Software Architecture

The flight firmware is developed in C++ within the ESP32 embedded framework using FreeRTOS. Core 0 executes high-frequency tasks: reading the MPU6050 via I2C at 400 kHz, calculating attitude roll and pitch via a complementary filter (α = 0.98), and computing PID motor outputs at 250 Hz. Core 1 manages asynchronous telemetry, polling the NEO-6M GPS module at 9600 baud via UART, sampling battery voltage via an internal ADC with resistor divider, and decoding 2.4 GHz RC pulse signals.

A watchdog timer monitors incoming RC pulses. If pulse train reception ceases for more than 1.0 second, or if the LiPo battery drops below 10.5 V, Core 1 asserts an emergency interrupt flag, switching the flight state machine from Manual Flight to Autonomous Return-to-Home. The navigation algorithm calculates bearing β and geodesic distance d to the latched Home Point using the Haversine trigonometric equations:

$$d = 2R \cdot \arcsin\left(\sqrt{\sin^2(\Delta\varphi/2) + \cos(\varphi 1)\cos(\varphi 2)\sin^2(\Delta\lambda/2)}\right)$$

$$\beta = \operatorname{atan2}(\sin(\Delta\lambda)\cos(\varphi 2),\ \cos(\varphi 1)\sin(\varphi 2) - \sin(\varphi 1)\cos(\varphi 2)\cos(\Delta\lambda))$$

III. HARDWARE-BASED SYSTEM

A. ESP32 Dev Board (Flight Controller)



Fig. 3. ESP32 microcontroller dev board.
Source: espressif.com/.../esp32-devkitc

The ESP32 Dev Board serves as the central flight computer. Featuring an Xtensa dual-core 32-bit LX6 processor running at 240 MHz, 520 KB internal SRAM, and 4 MB SPI flash, it delivers the computational bandwidth necessary for real-time PID loops and trigonometric navigation. Hardware PWM timers generate four synchronized motor signals on GPIOs 12, 13, 14, and 27 with sub-microsecond pulse fidelity.

B. NEO-6M GPS Module



Fig. 4. NEO-6M GPS module.
Source: u-blox.com/.../neo-6-series

The u-blox NEO-6M GPS module provides geographical positioning via a 50-channel tracking engine with a -161 dBm sensitivity. Interfaced via UART on GPIO 16 (RX) and GPIO 17 (TX), it provides real-time latitude, longitude, and ground speed at 1 Hz update rates, achieving a horizontal position accuracy of 2.5 meters Circular Error Probable (CEP).

C. MPU6050 6-DOF IMU Sensor



Fig. 5. MPU6050 6-DOF IMU sensor.
Source: invensense.tdk.com/.../mpu-6050

The MPU6050 sensor integrates a 3-axis MEMS accelerometer and 3-axis gyroscope with 16-bit analog-to-digital converters on a single silicon die. Interfaced with the ESP32 via I2C on GPIO 18 (SCL) and GPIO 19 (SDA), it tracks angular velocity up to ±2000°/s and gravitational acceleration up to ±8g, delivering essential angular data for leveling and counteracting external wind gusts.

D. 2.4 GHz RC Transmitter and Receiver



Fig. 6. 2.4 GHz RC receiver module.
Source: flysky-cn.com/.../ia6b

A 6-channel 2.4 GHz radio control system utilizes Automatic Frequency Hopping Digital System (AFHDS 2A) protocol to provide interference-free communication up to 500 meters. Channels 1 through 4 transmit Roll, Pitch, Throttle, and Yaw commands to the ESP32, while Channel 5 serves as a manual RTH toggle. Absence of frame pulses signals link disconnection.

E. 2200KV Brushless DC (BLDC) Motors



Fig. 7. 2200KV brushless DC motors.
Source: components101.com/.../a2212-brushless-motor

Four A2212 2200KV outrunner BLDC motors provide quadcopter propulsion. Operating on 11.1 V nominal power, each motor produces up to 800 g of thrust with matched 10-inch propellers, yielding a combined thrust of 3.2 kg. This provides a 2.9:1 thrust-to-weight ratio for responsive acceleration and strong wind resistance.

F. 30A Electronic Speed Controller (ESC)



Fig. 8. 30A Electronic Speed Controller (ESC).
Source: thingbits.in/.../30a-esc

Four 30A Electronic Speed Controllers regulate brushless motor phase commutation using high-current N-channel MOSFET H-bridges. Receiving 50–400 Hz PWM throttle signals from the ESP32, the ESCs deliver up to 30 A continuous (40 A burst for 10 s) current. SimonK firmware ensures linear throttle response and rapid motor speed transitions.

G. 11.1V 3S LiPo Battery (2200 mAh)



Fig. 9. 11.1 V 3S 2200 mAh LiPo battery.
Source: robu.in/.../orange-2200mah-3s-lipo

An 11.1 V (3S1P) 2200 mAh Lithium-Polymer battery pack serves as the primary energy reservoir. Delivering up to 55 A continuous current (25C discharge rating), it powers the heavy motor draws while maintaining flight times of 10 to 12 minutes. An onboard voltage divider allows the ESP32 ADC to monitor cell depletion in real time.

H. 5V 3A Battery Eliminator Circuit (BEC)



Fig. 10. 5V 3A Battery Eliminator Circuit (BEC).
Source: thingbits.in/.../5v-3a-ubec

A high-efficiency switching step-down buck converter (BEC) steps the 11.1 V battery voltage down to a clean, isolated 5.0 V DC rail at up to 3 A. This dedicated supply powers the ESP32, NEO-6M GPS, MPU6050, and RC receiver, protecting delicate digital logic from motor switching noise and transient voltage spikes.

I. F450 Drone Frame and Propellers



Fig. 11. F450 quadcopter drone frame.
Source: dji.com/.../flame-wheel-450

The airframe is an F450 quadcopter platform with a 450 mm motor wheelbase constructed from ultra-strength polyamide arms and a glass-fiber composite central chassis with an integrated power distribution board (PDB). Matched 1045 propellers (two clockwise and two counter-clockwise) cancel reactive yaw torque while generating smooth, balanced aerodynamic lift.

J. (Optional) SD Card Module



Fig. 12. MicroSD card telemetry logging module.
Source: arduino.cc/.../Reference/SD

An optional SPI-interfaced MicroSD card module functions as an onboard flight data recorder ("black box"). Logging at 10 Hz, it records GPS latitude, longitude, barometric/GPS altitude, battery voltage, PID error terms, and failsafe trigger states in CSV format for post-mission engineering analysis.

IV. WORKING OF THE SYSTEM

The operational lifecycle of the Return-to-Home drone follows a five-stage sequence: (1) GPS Fix Acquisition, (2) Normal Flight, (3) Failsafe Trigger, (4) Navigate Home, and (5) Approach and Land.

1) Acquire GPS Fix: Upon system power-on, the ESP32 initializes all peripherals and monitors the NEO-6M GPS module. The flight controller prevents motor arming until a minimum of 6 satellites are acquired with an HDOP < 1.5. Once confirmed, the system latches the current latitude and longitude as the immutable "Home Point" in memory.

2) Normal Flight: During standard operation, the pilot steers the quadcopter via the 2.4 GHz RC link. The ESP32 processes pilot stick inputs, samples the MPU6050 IMU, and executes PID attitude loops to maintain stable flight.

3) RTH Triggering: The failsafe engine monitors radio signal pulses and battery voltage. If the pilot activates the RC transmitter RTH switch, if RC pulses cease for > 1.0 s (lost link), or if battery voltage drops below 10.5 V, the ESP32 triggers the autonomous Return-to-Home state machine.

4) Navigate Home: Upon trigger, the drone ascends to a preset safety altitude (15 m) to clear obstacles. The ESP32 then calculates target bearing β to the launch site, yaws toward the home point, and adjusts forward pitch to cruise autonomously toward the stored coordinates at 5.0 m/s.

5) Approach and Land: When the GPS position enters a 3-meter radius geofence surrounding the launch site, the drone slows, halts forward pitch, and hovers for 5 seconds to stabilize. It then initiates controlled vertical descent at 0.5 m/s until touchdown is detected, cutting motor PWM signals and disarming safely.

V. PROTOTYPE TESTING AND RESULTS

Flight trials were conducted in an open suburban field in Wagholi, Pune, across ten experimental sorties simulating RC transmitter power cutoffs and forced low-battery triggers. Telemetry data confirmed consistent autonomous navigation and landing precision.

TABLE I. PROTOTYPE PERFORMANCE SUMMARY

Parameter	Observed Metric	Status
GPS Cold Start Fix Time	32–45 seconds	Optimal
Failsafe Trigger Response	1.1–1.3 seconds	Instant
Cruise Return Speed	4.8–5.8 m/s	Stable
Landing Accuracy (CEP)	1.2–1.8 meters	High Precision
Vertical Descent Velocity	0.5–0.7 m/s	Controlled
Battery Cutoff Trigger	10.48 V (±0.05 V)	Reliable
Overall RTH Success Rate	100% (10/10 trials)	Validated

VI. LIMITATIONS AND CHALLENGES

Key technical challenges include single-frequency GPS multipath degradation under dense foliage, barometric ground-effect turbulence during final touchdown, and magnetic compass deflection from high-current ESC wiring.

VII. FUTURE SCOPE

Future work will incorporate dual RTK-GPS for centimeter-level touchdown accuracy, ultrasonic/LiDAR obstacle avoidance sensors, downward optical flow for GPS-denied navigation, and AI vision-based landing pad detection.

VIII. CONCLUSION

The developed GPS-Based Return-to-Home Drone provides a reliable, cost-effective embedded failsafe architecture. By combining the ESP32 microcontroller with a NEO-6M GPS receiver and MPU6050 IMU, the system eliminates catastrophic flyaways and delivers dependable recovery across civilian UAV missions.

REFERENCES

[1] K. Alexis, G. Nikolakopoulos, and A. Tzes, "Model predictive quadrotor control: attitude, altitude and position experimental studies," *IET Control Theory & Applications*, vol. 6, no. 12, pp. 1812–1827, 2012.
[2] P. Castillo, R. Lozano, and A. E. Dzul, *Modelling and Control of Mini-Flying Machines*, London: Springer-Verlag, 2005.
[3] S. Bouabdallah, P. Murrieri, and R. Siegwart, "Design and control of an indoor micro quadrotor," in *Proc. IEEE Int. Conf. Robot. Autom. (ICRA)*, New Orleans, LA, 2004, pp. 4393–4398.
[4] M. W. Mueller, M. Hehn, and R. D'Andrea, "A relaxed barrier function approach to feedforward trajectory generation for quadrocopters," *IEEE Trans. Robot.*, vol. 31, no. 4, pp. 877–889, 2015.
[5] H. Chao, Y. Gu, and M. Napolitano, "A survey of optical flow techniques for UAV navigation applications," *Prog. Aerosp. Sci.*, vol. 83, pp. 62–72, 2016.
[6] R. Mahony, T. Hamel, and J.-M. Pflimlin, "Nonlinear complementary filters on the special orthogonal group," *IEEE Trans. Autom. Control*, vol. 53, no. 5, pp. 1203–1218, 2008.
[7] J. F. Vasconcelos, R. Cunha, C. Silvestre, and P. Oliveira, "A nonlinear position and heading filter for UAVs using IMU and GPS," in *Proc. 47th IEEE Conf. Decis. Control*, Cancun, Mexico, 2008, pp. 4040–4045.
[8] T. B. Schon, F. Gustafsson, and P.-J. Nordlund, "Marginalized particle filters for mixed linear/nonlinear state-space models," *IEEE Trans. Signal Process.*, vol. 53, no. 7, pp. 2279–2289, 2005.
[9] A. Nemra and N. Aouf, "Robust INS/GPS sensor fusion for UAV navigation using RKF," *IEEE Trans. Aerosp. Electron. Syst.*, vol. 46, no. 2, pp. 589–604, 2010.
[10] D. Scaramuzza et al., "Vision-controlled micro flying robots: from system design to autonomous navigation," *IEEE Robot. Autom. Mag.*, vol. 21, no. 3, pp. 26–40, 2014.
[11] G. Hoffmann, H. Huang, S. Waslander, and C. Tomlin, "Quadrotor helicopter flight dynamics and control: Theory and experiment," in *Proc. AIAA Guid. Navig. Control Conf.*, Hilton Head, SC, 2007, pp. 1–20.
[12] u-blox AG, "NEO-6 u-blox 6 GPS Modules Data Sheet," Document UBX-14004472, Thalwil, Switzerland, 2014.
[13] InvenSense Inc., "MPU-6000 and MPU-6050 Product Specification Revision 3.4," Document PS-MPU-6000A-00, Sunnyvale, CA, 2013.
[14] Prof. V. B. Takale, S. Mohite, V. Jadhav, V. Pawar, and M. Amale, "Autonomous Return-to-Home (RTH) Quadcopter Drone Using GPS and Embedded Inertial Navigation," Tech. Rep., Dept. E&TC, JSPM's BSP, Pune, India, 2026.

BIOGRAPHIES



Prof. V. B. Takale is a Lecturer in the Department of E&TC, JSPM's BSP, Wagholi, Pune (e-mail: vbtakale_entc@jspmbspoly.edu.in). He possesses extensive teaching and research expertise in embedded systems, microcontroller architectures, industrial automation, and wireless telemetry engineering.



Suyash Mohite is with the Department of E&TC, JSPM's BSP, Wagholi, Pune (e-mail: suyashmohite45@gmail.com). His technical domain includes autonomous unmanned aerial vehicles, embedded control systems, C++ firmware development, and satellite-guided navigational algorithms.



Vedant Jadhav is with the Department of E&TC, JSPM's BSP, Wagholi, Pune (e-mail: jadhavvedant655@gmail.com). His focus encompasses flight dynamics, inertial measurement sensor fusion, real-time operating systems (FreeRTOS), and multirotor stability enhancement.



Vivek Pawar is with the Department of E&TC, JSPM's BSP, Wagholi, Pune (e-mail: vivekp9006@gmail.com). His interests center on avionics hardware integration, brushless propulsion systems, electronic speed control modulation, and failsafe recovery architectures.



Manish Amale is with the Department of E&TC, JSPM's BSP, Wagholi, Pune (e-mail: amalemanish10@gmail.com). His areas of interest include radio-frequency telecommunications, telemetry black-box data logging, power distribution networks, and embedded IoT applications.